

# Supporting Information

## MRI relaxivity enhancement of gadolinium oxide nanoshells with controllable shell thickness

Jinchang Yin,<sup>‡a</sup> Deqi Chen,<sup>‡b</sup> Yu Zhang,<sup>c</sup> Chaorui Li,<sup>a</sup> Lizhi Liu<sup>d</sup> and Yuanzhi Shao<sup>\*,a</sup>

---

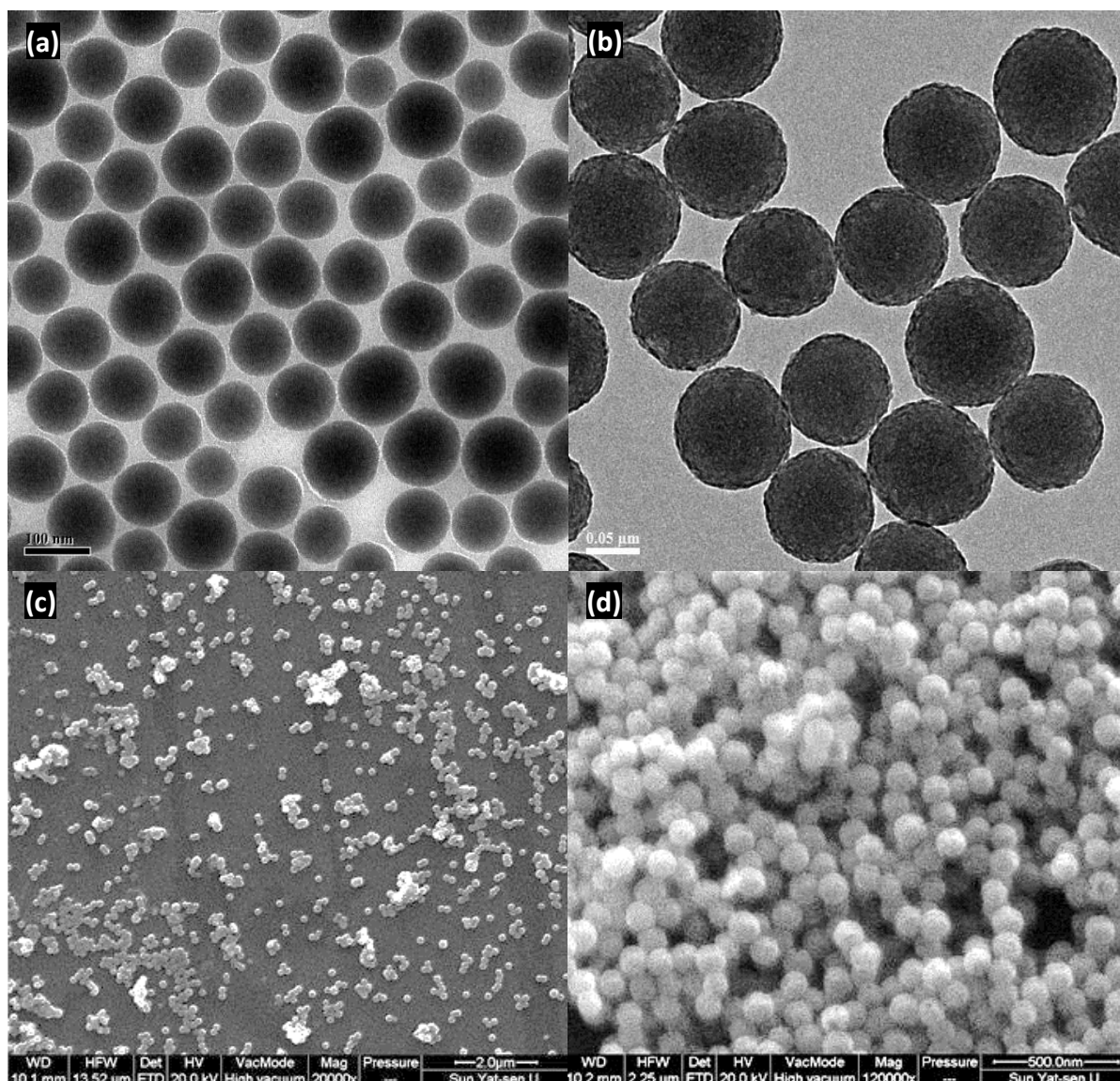
*a.* School of Physics, State Key Laboratory of Optoelectronic Materials and Technologies, Sun Yat-sen University, Guangzhou, 510275, P. R. China. E-mail: stssyz@mail.sysu.edu.cn

*b.* Medical Physics Graduate Program, Duke Kunshan University, Kunshan 215316, P. R. China.

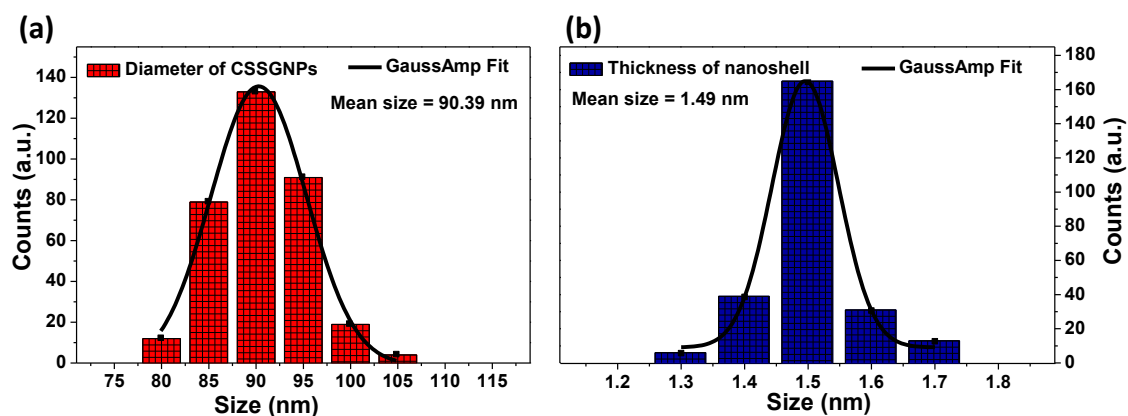
*c.* Department of Pathology, Sun Yat-sen University Cancer Center, State Key Laboratory of Oncology in South China, Collaborative Innovation Center for Cancer Medicine, Guangzhou 510060, P. R. China.

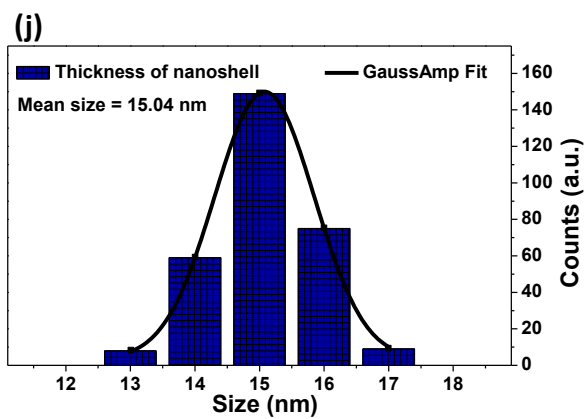
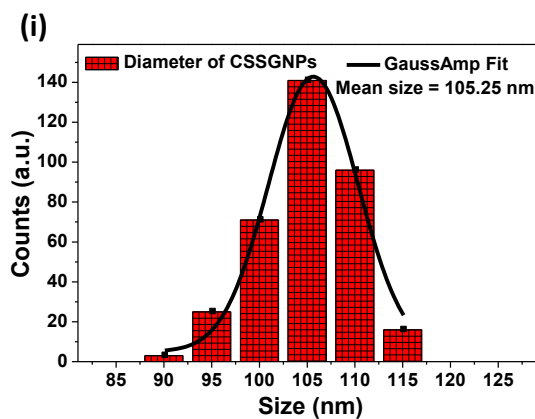
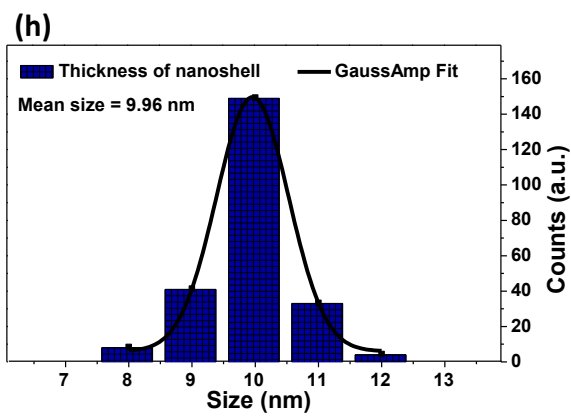
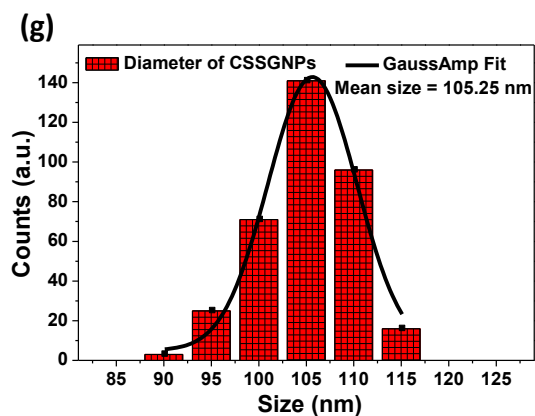
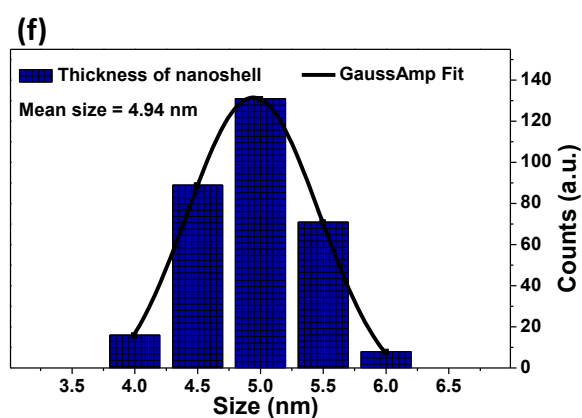
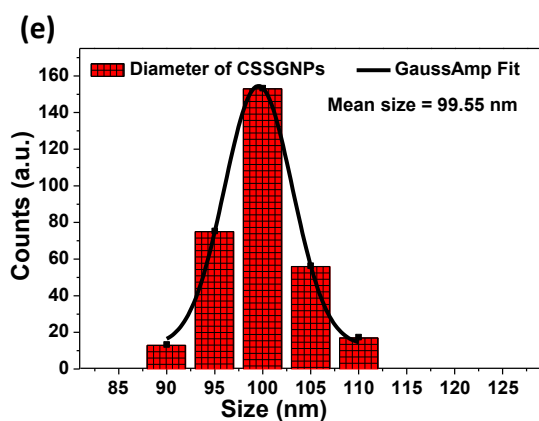
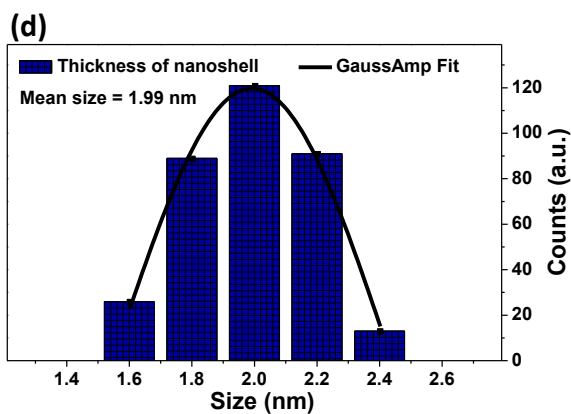
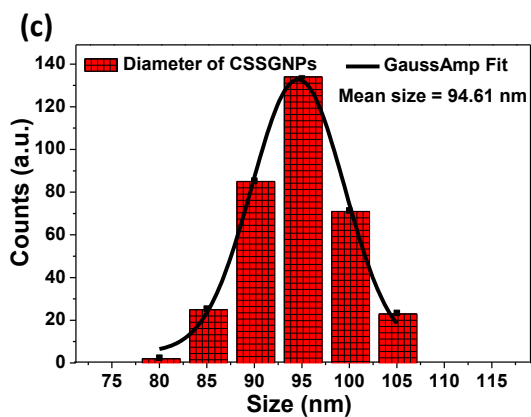
*d.* Center of Medical Imaging and Image-guided Therapy, Sun Yat-sen University Cancer Center, State Key Laboratory of Oncology in South China, Collaborative Innovation Center for Cancer Medicine, Guangzhou 510060, P. R. China.

<sup>‡</sup> Jinchang Yin and Deqi Chen contributed equally to this work.



**Fig. S1** (a, b) Wide-view TEM images of typical silica nanospheres and core-shelled silica-Gd<sub>2</sub>O<sub>3</sub> nanoparticles (1.5 nm shell) in relatively low magnifications. (c, d) Wide-view SEM images of the core-shelled silica-Gd<sub>2</sub>O<sub>3</sub> nanoparticles (1.5 nm shell) in different magnifications.





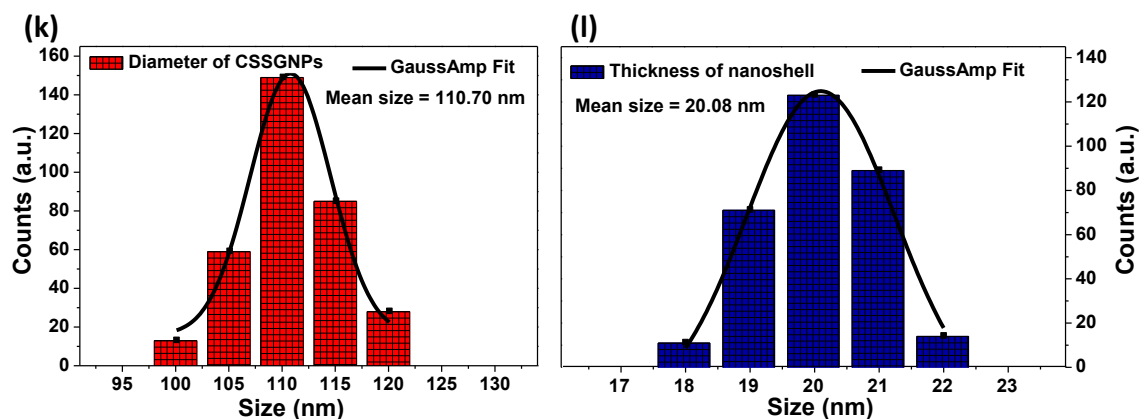


**Fig. S2** Size distribution histograms of core-varied shell structured nanoparticles. (a, c, e, g, i, k) The mean diameters of core-shelled nanoparticles (b, d, f, h, j, l) The mean thickness of varied nanoshells. Both diameter and thickness were measured from 250 – 300 recognizable particles randomly chosen from some TEM images and obtained via GaussAmp fits.

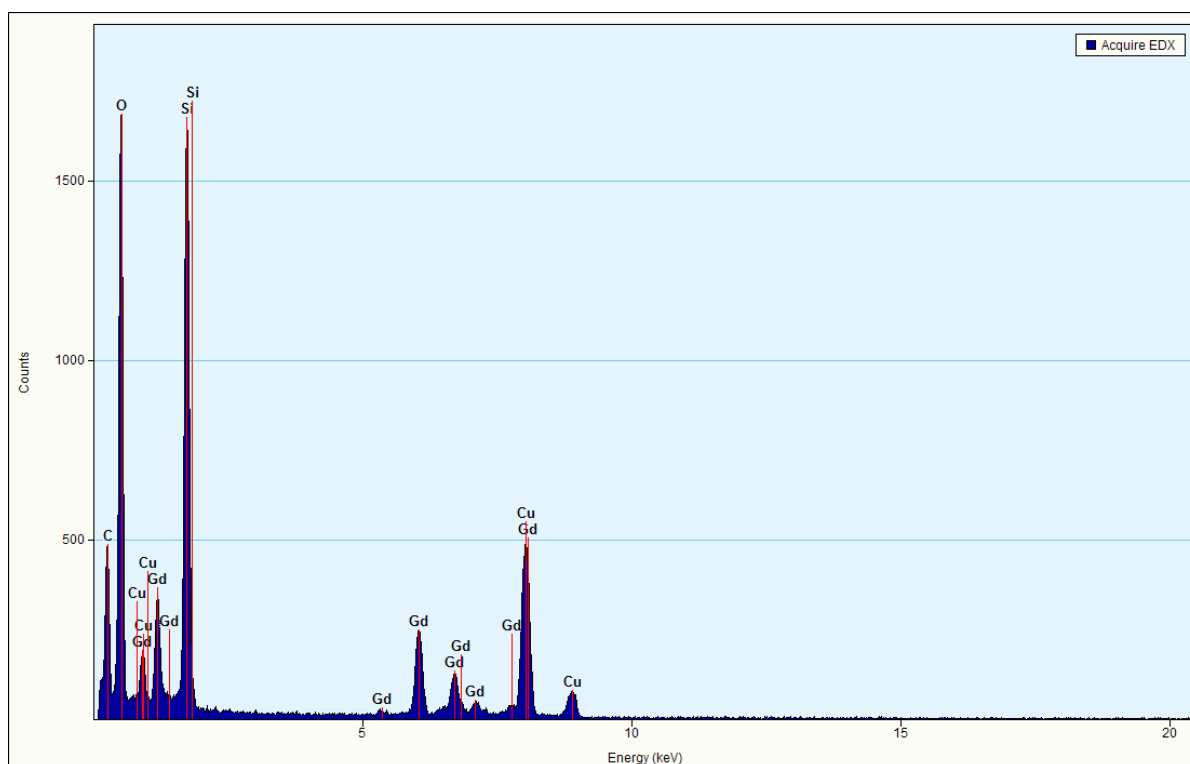


**Fig. S3** Energy-dispersive X-ray (EDX) spectroscopy of the core-shelled silica-Gd<sub>2</sub>O<sub>3</sub> nanoparticles (1.5 nm shell) in small-area detection with 300 kV voltage.

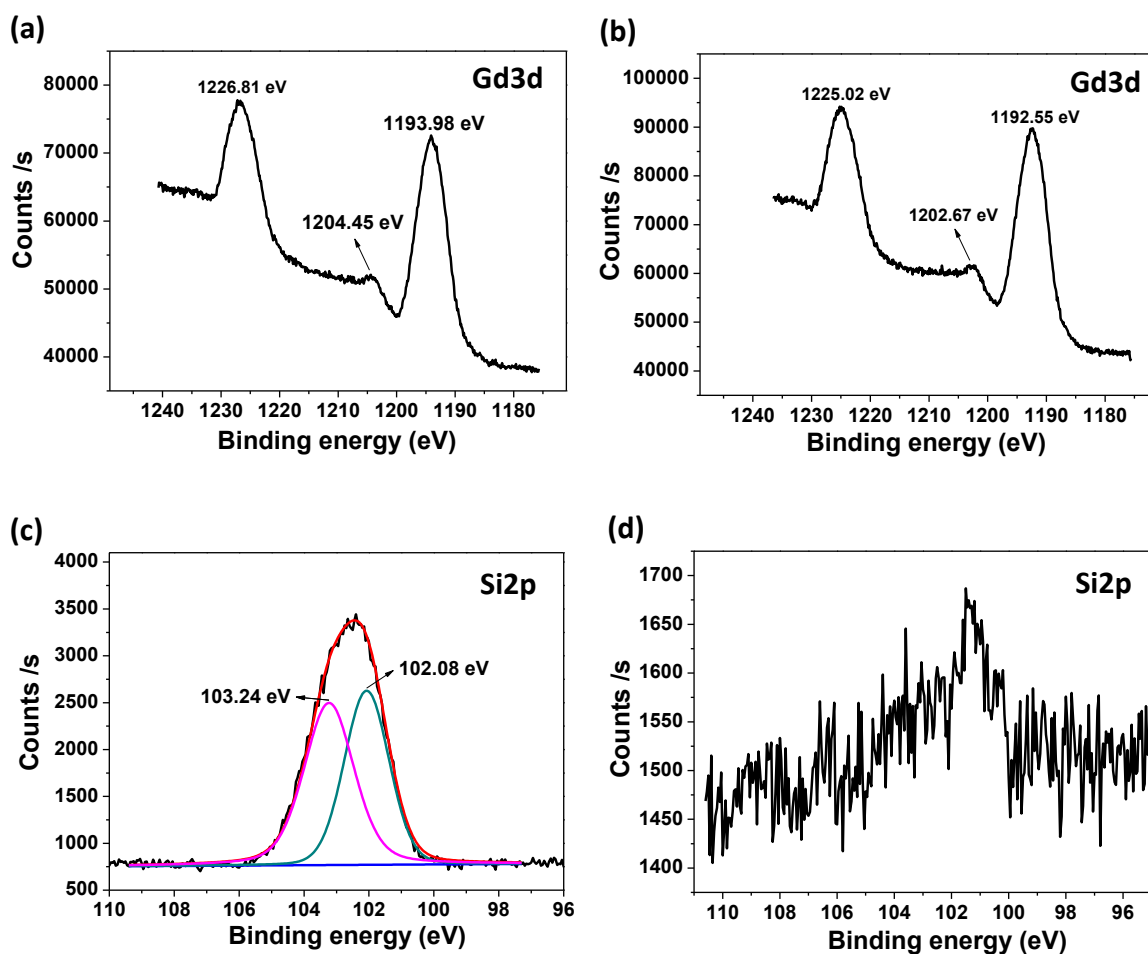
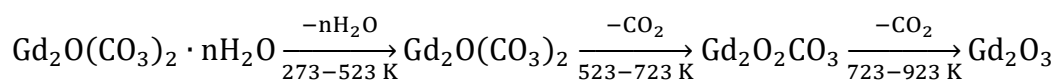


**Fig. S4** High-resolution X-ray photoelectron spectroscopy (XPS) patterns of the core-shelled nanoparticles. (a) Gd3d XPS pattern of core-thin shelled nanoparticles (1.5 nm). The peaks assigned to Gd3d<sub>3/2</sub>, and Gd3d<sub>5/2</sub> were detected at the binding energy of around 1226.81 eV and 1193.98 eV. The peak at 1204.45 eV is the satellite peak of Gd3d<sub>5/2</sub>. (b) Gd3d XPS pattern of core-thick shelled nanoparticles (20 nm). The peaks at 1225.02 eV and 1192.55 eV are ascribed to the surface Gd3d<sub>3/2</sub>, and Gd3d<sub>5/2</sub>. The peak at 1202.67 eV is the satellite peak of Gd3d<sub>5/2</sub>. (c) Si2p XPS pattern of core-thin shelled nanoparticles (1.5 nm). The peak is deconvoluted into two bands: one arises from the Si-O-Si siloxane bonds of silica structure (103.24 eV); the other is attributed to the formation of Si-O-Gd bonds (102.08 eV). (d) Si2p XPS pattern of core-thick shelled nanoparticles (20 nm).



**Scheme R1** Flow chart of the evolution of the shell phase composition in annealing process. we have discussed XRD fitting curves carefully. XRD spectra (Fig. 3b-3c) show the phase compositions of the as-prepared nanopowders after annealing at 523, 723 and 923 K, respectively, which can be reflected on TG-DTG patterns (Fig. 3a).

At 523 K, free water almost disappeared. Thus, the spectrum of XRD has a good signal to noise ratio. But some binding water molecules still exist in the nanoshell. The peaks of the spectrum were exactly indexed with that of gadolinium oxide carbonate hydrate (PDF 43-0604), formulated with  $\text{Gd}_2\text{O}(\text{CO}_3)_2 \cdot n\text{H}_2\text{O}$ . Around 625K, most water molecules were eliminated, and some carbon dioxide molecules were decomposed from  $\text{Gd}_2\text{O}(\text{CO}_3)_2 \cdot n\text{H}_2\text{O}$ .

At 723 K, apart from the corresponding XRD peaks of cubic gadolinium oxide, there were some diffraction peaks which are consistent with that of hexagonal gadolinium carbonate peroxide  $\text{Gd}_2\text{O}_2\text{CO}_3$  (PDF#23-0257), indicating two crystal materials existed simultaneously. Moreover, there were amorphous silica and  $\text{Gd}_2\text{O}(\text{CO}_3)_2$  whose signals were covered by crystal signal. It also demonstrated that the amorphous  $\text{Gd}_2\text{O}(\text{CO}_3)_2$  turns into crystallographic  $\text{Gd}_2\text{O}_2\text{CO}_3$  by decomposing one  $\text{CO}_2$  molecule. Then hexagonal  $\text{Gd}_2\text{O}_2\text{CO}_3$  took off another  $\text{CO}_2$  and became cubic  $\text{Gd}_2\text{O}_3$ .

When the temperature rose up to 923 K, all carbon dioxide molecules were eliminated. And it can be determined that the nanoshell consist of pure cubic gadolinium oxide because the peaks of spectrum are in good agreement with that of standard cubic  $\text{Gd}_2\text{O}_3$  (PDF#65-3181) and no impurity was detected. In order to ensure the purity of nanoshell crystals, 1023 K temperature was adopted for annealing in our experiment.

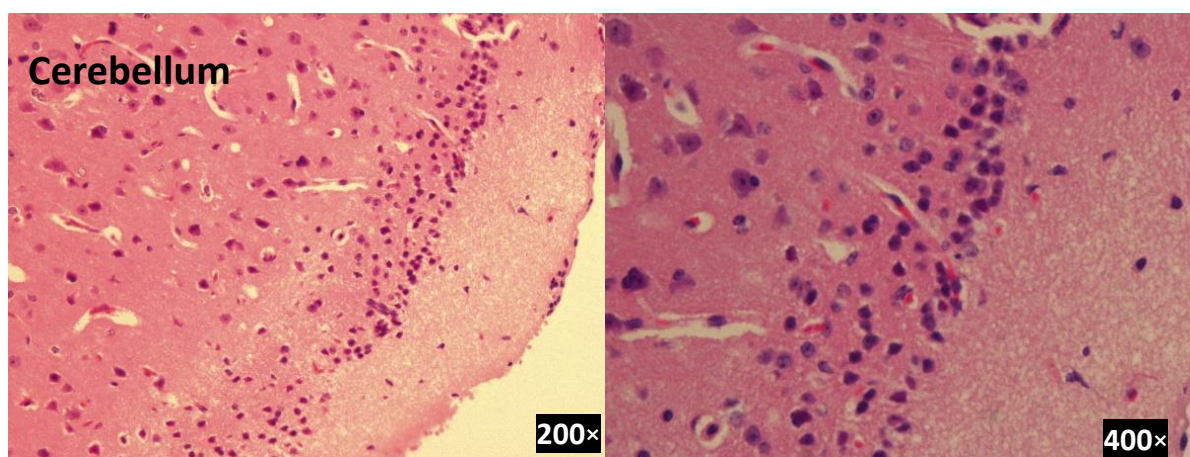


**Fig. S5** H&E stained images of the tissue of cerebellum, harvested from mice at 24 h after administration of  $10 \mu\text{mol kg}^{-1}$  CSSGNPs (1.5 nm shell) PBS solutions, observing under a light microscope at 200 and 400  $\times$  magnification.

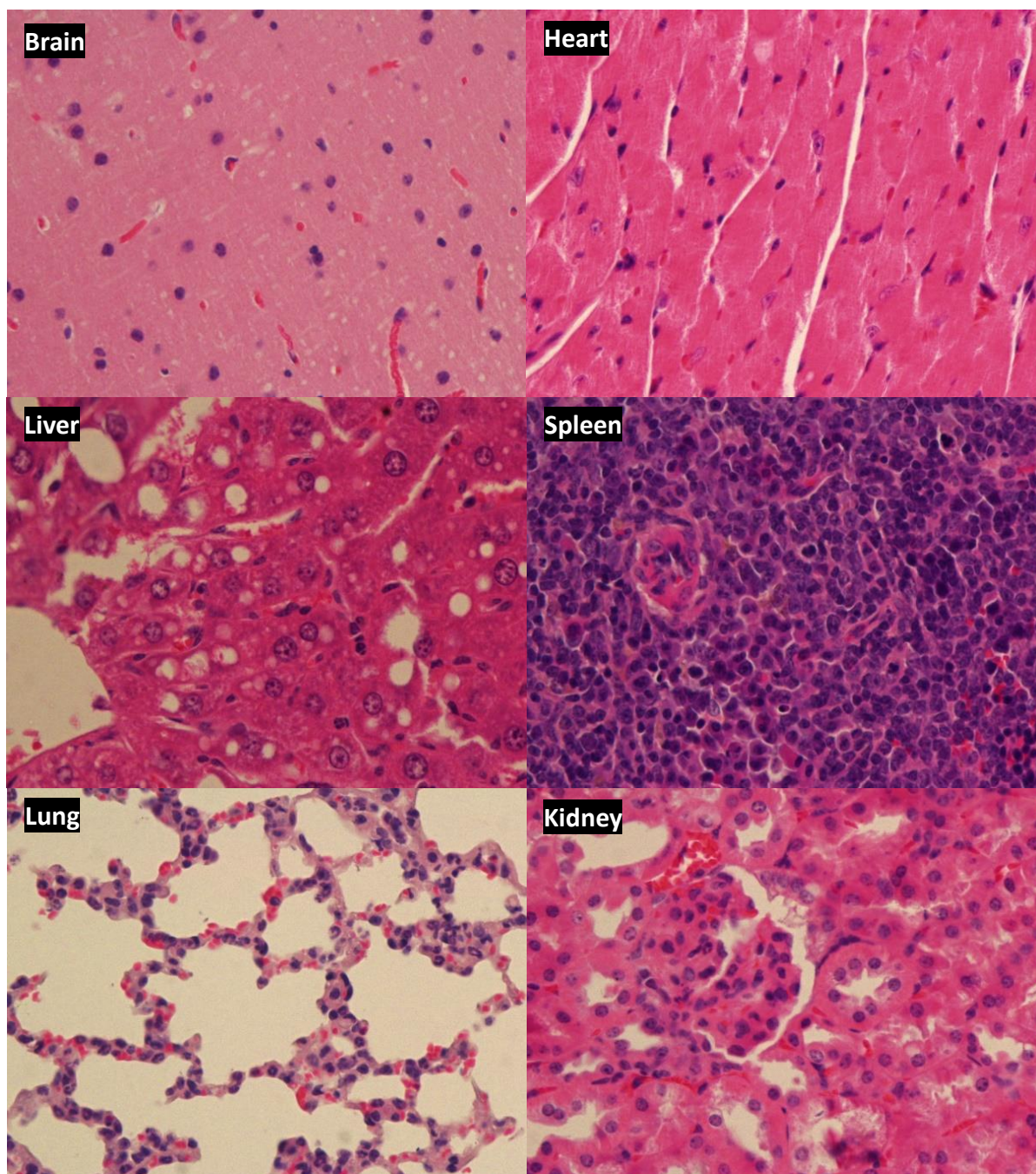


**Fig. S6** H&E stained images of typical tissues including brain, heart, liver, spleen, lung and kidney, harvested from mice at 24 h after administration of  $10 \mu\text{mol kg}^{-1}$  CSSGNPs (1.5 nm shell) PBS solutions, observing under a light microscope at  $400 \times$  magnification.

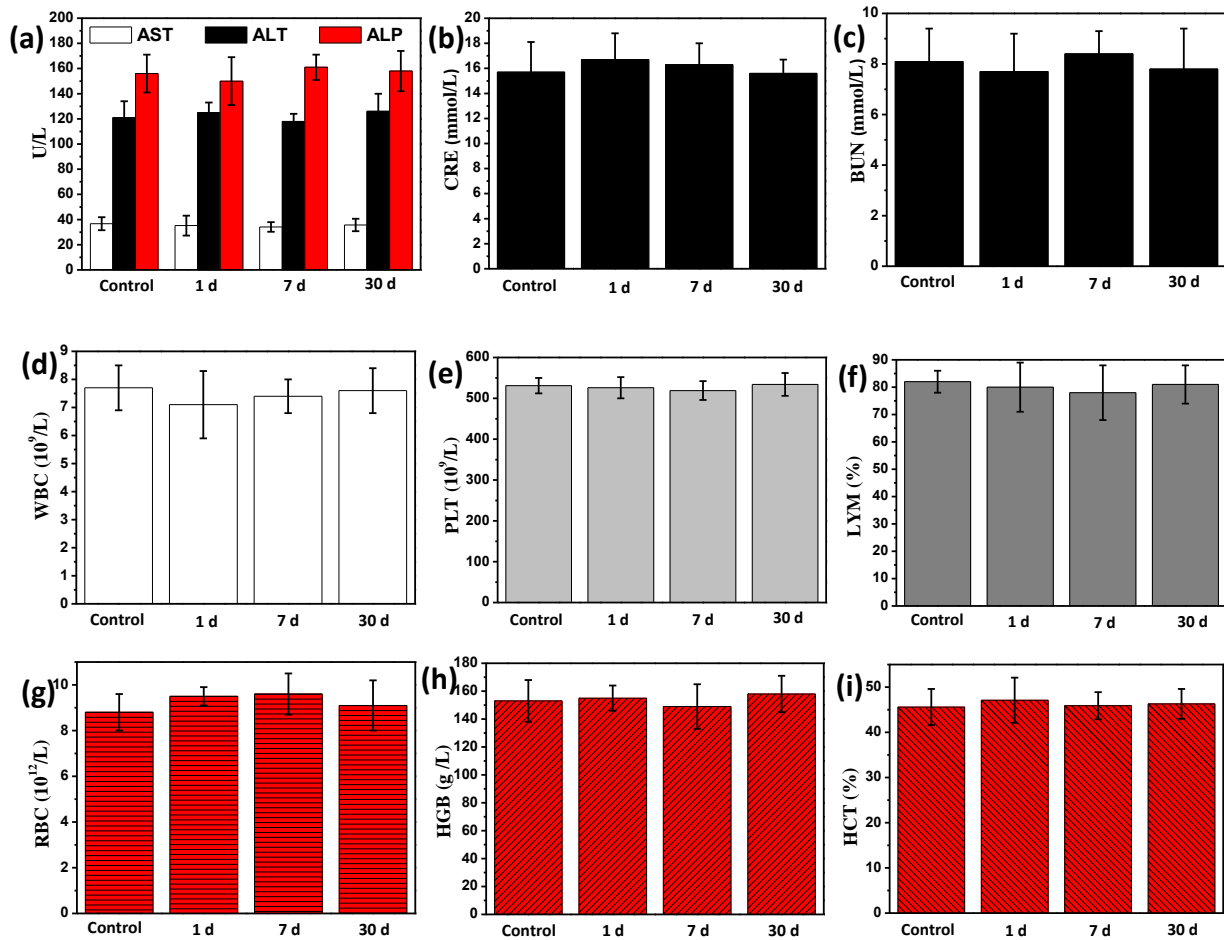


**Fig. S7** Hematological data (n=5) obtained from healthy Kunming mice after the intravenous administration of the CSSGNPs (1.5 nm shell) PBS solutions ( $10 \mu\text{mol kg}^{-1}$ , mean  $\pm$  SD, n = 5) at 1, 7, and 30 days and pure PBS solutions as control. (a) The blood biochemistry levels of alanine transaminase (ALT), aspartate transaminase (AST) and alkaline phosphatase (ALP) as liver function indicators. (b, c) Creatinine (CRE) and blood urea nitrogen (BUN) levels in the blood indicating kidney functions. The complete blood panel data involving (d) white blood cells (WBC), (e) platelets (PLT), (f) lymphocyte (LYM), (g) red blood cells (RBC), (h) hemoglobin (HGB) and (i) hematocrit (HCT). Other blood parameters such as mean corpuscular hemoglobin (MCH), mean corpuscular hemoglobin concentration (MCHC), mean corpuscular volume (MCV), red blood cell distribution width (RDW), mean platelet volume (MPV), platelet distribution width (PDW), thrombocytocrit (PCT), which are not shown here, also fell well within normal ranges compared to the control group.